

Dynamic-mechanical behavior of polyethylenes and ethene-/ α -olefin-copolymers. Part I. α' -Relaxation

Florian J. Stadler*, Joachim Kaschta, Helmut Münstedt¹

Department of Materials Science, Institute of Polymer Materials, Friedrich-Alexander University Erlangen-Nürnberg, Martensstrasse 7, D-91058 Erlangen, Germany

Received 17 March 2005; received in revised form 19 July 2005; accepted 29 July 2005

Available online 19 August 2005

Abstract

Polyethylenes and polyethylene/ α -olefin-copolymers covering a range in crystallinity between 12 and 85% were investigated by means of dynamic-mechanical measurements between -145 °C and their melting point. From the temperature and frequency dependence of the complex modulus α' -, α -, β - and γ -relaxations were analyzed. The α' -relaxation was discovered in all HDPE-, LDPE- and LLDPE-samples but not in plastomer- and elastomer-samples. The activation energies (30–140 kJ/mol) of this relaxation were found to decrease with increasing crystallinity. The α' -transition temperature at a fixed frequency rises with increasing degree of crystallinity and tends to reach the melting point when approaching the fully crystalline state. Thus, it is concluded that the α' -relaxation originates from the interface between crystal lamellae and amorphous interlamellar regions. By extrapolation of the storage modulus to the amorphous state the entanglement molar mass was calculated as 2300 g/mol for a completely amorphous polyethylene/ α -olefin-copolymer.

© 2005 Elsevier Ltd. All rights reserved.

Keywords: Polyethylene; Ethene-/ α -olefin-copolymer; Activation energy

1. Introduction

Solid-state mechanical properties of polymers are strongly influenced by molecular motions under the given thermodynamic conditions and the applied mechanical stress. Molecular motions can effectively be studied by means of dynamic-mechanical experiments. The temperature at which a molecular motion at a certain frequency freezes in is called relaxation or transition temperature. In a dynamic-mechanical experiment at constant frequency each transition is characterized by a maximum of the loss factor $\tan \delta$ if plotted as a function of temperature. The knowledge of the transitions of a material is one key to understand the mechanical properties of a polymer.

In polyethylenes and polyethylene/ α -olefin-copolymers, it is common to label the transitions with decreasing transition temperatures as α -, β - and γ -transition [1].

In most papers on the dynamic-mechanical properties of polyethylene and its copolymers measurements are found at only one constant frequency, typically 1 Hz, for a constant rate of temperature change in a temperature range from -150 °C to the melting point. Papers describing the frequency dependence are scarce [2,3]. Only few papers deal with dynamic-mechanical properties at temperatures below -150 °C [4,5]. In this temperature range, the so-called δ - and ϵ -relaxation occurs.

The α -transition is observed in all semi-crystalline polymers [2]. In polyethylenes this relaxation is split into two overlapping processes, which are both related to the crystalline phase [2,3]. Two different ways of designating the two α -relaxations are found. Nitta and Tanaka [2] label the two α -relaxations with the higher transition temperature as α_2 -relaxation and the lower as α_1 -relaxation. Matthews et al. [3] and Simanke et al. [6] call these relaxations α' - and α -relaxation, respectively. As the mechanisms of the α -/ α_1 -relaxation are believed to be the same as in other semi-crystalline polymers the nomenclature of Matthews et al. and Simanke et al. is used.

The origin of the α' -relaxation is attributed by Nitta and Tanaka [2] to interface processes at the boundary between crystalline and amorphous phase. The authors state that the

* Corresponding author. Tel.: +49 9131 852 7751; fax: +49 9131 852 8321.

E-mail address: florian.stadler@ww.uni-erlangen.de (F.J. Stadler).

¹ Tel.: +49 9131 852 7604.

process is an interlamellar slip process or some kind of grain boundary phenomenon. The α' -transition is observed at temperatures above the α -transition. Its activation energy is reported to be approximately 80 kJ/mol. According to Takanayagi and Matsuo [7], this relaxation is very sensitive to orientations of the lamellae.

This three-part article deals with the influence of the cooling conditions, comonomer type and content on the α' -, α -, β - and γ -transition. These parameters are the main factors influencing on the morphology of the samples. The main topic of this paper is the α' -transition which is seldom described in literature. One reason for that is the very low intensity of the α' -transition when measured at constant frequency as a function of temperature. Due to the ample results, this article is split into three parts each dealing with a different transition. Part II deals with the α - and β -transition [9] while part III covers the γ -transition [10].

As the results will be related to the morphology of the samples the dependence of the crystal morphology on crystallinity is briefly reviewed.

Bensason et al. [8] describe four different crystalline morphologies observed in polyethylene and ethylene/ α -olefin copolymers:

- Type IV: Highly crystalline, i.e. crystallinity $x > 55\%$, highly lamellar crystallites, found in HDPE.
- Type III: Medium crystalline, $40 < x < 55\%$, lamellar crystallites, found in LLDPE.
- Type II: Low crystalline, $30 < x < 40\%$, mixture of bundle and lamellar crystallites, found in plastomers.
- Type I: Almost amorphous, $x < 30\%$, bundle crystallites, found in elastomers.

2. Experimental

2.1. Materials, sample preparation, thermal and molecular characterization

The α' -relaxation was investigated for a number of commercially available grades. The designation of the samples is chosen according to the producers' specification (HDPE, LLDPE, LDPE) together with a number. Their characteristic data are given in Tables 1 and 2. The molar mass distribution and LCB-content was measured by high temperature size exclusion chromatography (HT-SEC) (Waters, 150 C) with coupled multi angle laser light scattering MALLS (Wyatt, Dawn EOS). The numbers of LCB/molecule in Table 2 were calculated according to the Zimm-Stockmayer model for three-functional branching points [11].

The melting point was measured on samples of about 10 mg by DSC (TA Instruments, DSC 2920) using the maximum of the melting peak at a heating rate of 10 K/min. As the measurement of the crystallinity by DSC is prone to

errors the crystallinity x_v was calculated from the density ρ ($\rho = 1/v$, v —specific volume) using the equation

$$x_v = \frac{v_a - v}{v_a - v_c} \quad (1)$$

with $v_c = 1.000 \text{ cm}^3/\text{g}$ and $v_a = 1.170 \text{ cm}^3/\text{g}$ for crystalline and amorphous regions, respectively, [12]. The density was measured on three different samples. Its standard deviation is between 0.06 and 0.35%. The error in the crystallinity (standard deviation of the density measurements) is below 3%. The error of the melting point is around 1 K.

The comonomer content was calculated from the number of $\text{CH}_3/1000 \text{ C}$ obtained by FT-IR-Spectroscopy (Nicolet Magna 750). To determine the number of $\text{CH}_3/1000 \text{ C}$ the intensity of the $\delta\text{-CH}_3$ -band (1376 cm^{-1}) was measured in extinction [13]. From the ratio of the $\delta\text{-CH}_2$ -band (1368 cm^{-1}) to the $\delta\text{-CH}_3$ -band the comonomer type was evaluated [14] if not given by the manufacturer. The comonomer content n was calculated according to Eq. (2).

$$n = \frac{2(c - c_{\text{EG}})}{100 - d(c - c_{\text{EG}})} \times 100 \text{ mol}\% \quad (2)$$

with

$$c_{\text{EG}} = \frac{2 + k}{2000P_w}$$

with c , number of methyl groups/1000 carbons (spectroscopic reading); d , number of carbons in a short chain branch (comonomer length-2) (C), e.g. octene 6; k , number of long chain branches/molecule (–); P_w , weight average degree of polymerization ($M_w/28 \text{ g/mol}$) (–); c_{EG} , number of methyl end groups of backbone and long chain branches.

This equation assumes a CH_3 -group at each chain end (backbone, short-chain branch (SCB) and long-chain branch (LCB)). To calculate the comonomer content the number of methyl groups being located at the end of the SCBs has to be divided by the number of backbone carbons. Therefore the end groups of the main chain and the LCBs (CH_3 ,_{EG}) have to be deducted by taking the weight average degree of polymerization ($P_w = M_w/28 \text{ g/mol}$) and the average number of LCBs/molecule (k) into account. Omitting the methyl end groups of the backbone will lead to values of the comonomer content, which are about 0.03–0.3 mol% too high when assuming molar masses M_w between 30 and 1000 kg/mol. The LCB-content may account for even more methyl end groups than the backbone end groups as the highly branched products were found to contain more than 30 LCBs/molecule. The number of backbone carbons has to be calculated by deducting the number of carbons located in the SCBs (C_{SCB}) from the total number of carbons in the sample.

The samples were molded in a laboratory hot press (Vogt, LaboPress 200 T) at $180 \text{ }^\circ\text{C}$ for 6 min at a pressure of 300 bar. The cavity dimensions were $2 \times 10 \times 30 \text{ mm}^3$. Two cooling methods were used to obtain different morphologies:

Table 1
Melting temperatures, densities and crystallinities for the resins investigated

Name	Quenched samples			Slowly-cooled samples		
	Melting temperature T_m (°C)	Density (g/cm ³)	Crystallinity x_v (%)	Melting temperature T_m (°C)	Density (g/cm ³)	Crystallinity x_v (%)
HDPE 1	139.6	0.947	70	139.4	0.970	80
HDPE 2	135.0	0.940	63	135.1	0.949	68
HDPE 3	133.2	0.937	61	133.6	0.948	68
HDPE 4	133.9	0.933	58			
LLDPE 1	124.1	0.919	48			
LLDPE 2	115.3/123.0 ^a	0.915	45			
LDPE 1	110.4	0.915	45	110.4	0.919	48
LLDPE 3	115.8	0.913	44			
LLDPE 4	112.2	0.910	42			
LLDPE 5	106.7	0.904	37			
LLDPE 6	101.4	0.898	33			
LLDPE 7	100.4	0.898	33	100.9	0.901	35
LLDPE 8	97.8	0.897	32	96.9	0.902	36
LLDPE 9	94.0	0.896	32			
LLDPE 10	97.1	0.893	30			
LLDPE 11	44.1/63.5 ^a	0.871	13			

^a Two discrete melting maxima were observed, for further analysis the average of the two values was taken.

1. Slow-cooling method: The pressed sample is cooled to ambient temperature over a period of approximately 6 h under constant pressure in the hot press.
2. Quenching method: The pressed sample is immediately immersed into ice water, leading to a cooling time around 3 s to sub-ambient temperatures.

2.2. DMTA-measurements

The DMTA-measurements (Rheometric Scientific, DMTA IV, with a liquid nitrogen cryogenic unit) were performed in three point bending with a span of 22 mm. The samples were between 1.8–1.95 mm in height and 9.7–9.9 mm in width.

Table 2
Molecular characteristics

Name	Comonomer ^a	Comonomer content (%) ^b	CH ₃ /1000 C ^c	Catalyst ^d	M_w (kg/mol)	M_n (kg/mol)	M_w/M_n	LCB/molecule
HDPE 1	–	–	0	ZN	170	33.8	5.0	0
HDPE 2	B	1.14 ± 0.41	6.4	ZN	463	18.5	25.0	22.5
HDPE 3	O	2.33 ± 0.46	11	ZN	369	10.1	36.7	0.5
HDPE 4	–	–	0	m	196	65.3	3.0	0
LLDPE 1	O	3.25 ± 0.49	15	ZN	135	40	3.4	0
LLDPE 2	O	2.77 ± 0.48	13	ZN	124	38.8	3.2	0
LDPE 1	–	4.82 ± 0.48 ^e	22	–	345	31.4	11.0	31.1
LLDPE 3	H	2.36 ± 0.44	11.5	m	111	48.3	2.3	0
LLDPE 4	O	2.63 ± 0.47	12.6	m	85	45.7	1.9	0.6
LLDPE 5	O	4.27 ± 0.52	20.2	m	69	30.0	2.3	4
LLDPE 6	O	5.90 ± 0.56	25.5	m	94	42.7	2.2	1
LLDPE 7	H	5.84 ± 0.50	26.4	m	110	50.0	2.2	0
LLDPE 8	O	6.18 ± 0.57	26.6	m	89	38.7	2.3	1
LLDPE 9	B	7.56 ± 0.46	35.4	m	110	44	2.5	0
LLDPE 10	O	4.78 ± 0.53	21.3	m	91	32.5	2.8	0.6
LLDPE 11	O	11.40 ± 0.50	51.6	m	135	67.5	2.0	2

^a B, butene; H, hexene; O, octene.

^b Measured by FT-IR.

^c Calculated according to (3) error ± 2 CH₃/1000 C.

^d ZN, Ziegler–Natta-catalyst; m, metallocene catalyst.

^e Comonomer content calculated assuming ethyl short chain branches.

The method uses frequency sweeps (within the linear-viscoelastic regime) of two different samples. Sample 1 is cooled down to $-140\text{ }^{\circ}\text{C}$. In our case, a frequency sweep between 0.0063 and 10 Hz with five frequencies per decade is employed. After each test, the temperature is set 10 K higher. To achieve thermal equilibrium conditions the next frequency sweep is started after a waiting time of 600 s. This procedure is repeated continuously until the temperature is just below the melting point. Sample 2 is treated the same way but starts at $-145\text{ }^{\circ}\text{C}$ so that a complete frequency sweep is available all 5 K. The data resulting from arbitrarily chosen frequencies, typically 1 Hz, are then plotted as a function of the temperature.

With this method it is possible to efficiently measure the characteristic frequency–temperature dependence of all transitions. The peak temperature at each frequency is numerically determined by setting the first derivative with respect to temperature (mean of the difference quotient of three neighboring data points) of the data to zero.

3. Results and discussion

3.1. Thermal and molecular characterization

As shown in Table 2 some of the products are narrowly distributed metallocene-types with M_w/M_n around 2 while others are very broad with M_w/M_n up to 36. The materials HDPE 2 and LDPE 1 (with a broad molar mass distribution) are long-chain branched while HDPE 3 is only slightly branched. Especially their high molar masses carry the LCB. Some of the metallocene-types are also long-chain branched but to a much lesser extent than the resins with a broad molar mass distribution. From the calculated values it can be concluded that two of the resins with a broad molar mass distribution (HDPE 2, LDPE 1) carry at least 10-times as many LCBs as the narrowly distributed ones.

Differences in the melting point T_m between the two different cooling methods are below 1 K (Table 1)—the thermal resolution of the DSC—therefore, the melting temperature is assumed to be unaffected by the thermal history. Quenching the samples lowers the crystallinity by 3–12% (Table 1).

The cubic root of the volumetric crystallinity, later on called ‘linear crystallinity’ $x_v^{1/3}$, was chosen as a non-dimensional measure for the crystal morphology. The physical meaning of this measure is that it is the amount of crystalline phase along any arbitrary straight line through the sample which makes it proportional to the crystal dimensions.

The molecular background can be understood by looking into crystallization mechanisms. It is well established that the melting point depends on the perfection of the crystallites. A high crystallite perfection is reflected in more stable and larger crystallites. A measure of the perfection of the crystallites is the lamella thickness. For the

melting point T_m a linear dependence on the lamella thickness l_c is found by Popli et al. [19] on quenched and slowly-cooled samples.

When analyzing the lamella thickness l_c as a function of $x_v^{1/3}$ according to the data of Popli et al. [19] two regimes are evident. At low values of $x_v^{1/3}$, l_c is constant. At linear crystallinities $x_v^{1/3}$ above 0.75 (crystallinity $x_v > 42\%$) a linear dependence of l_c on $x_v^{1/3}$ is detected. The crystallinity of 42% is approximately the border between a type II (bundle and lamellar) and a type III (lamellar) morphology. Because a purely lamellar structure no longer exists below a crystallinity of 42%, this correlation fails for $x_v < 42\%$.

As it is not simple to measure the lamella thickness, the linear crystallinity is adopted as an indirect quantity, which is easy to determine.

In Fig. 1, the linear crystallinity is plotted as a function of the melting point for slowly cooled and quenched samples. It increases linearly with the melting temperature having the same slope for the quenched and slowly-cooled samples. The difference in the crystallinity between quenched and slowly-cooled samples as a function of the melting temperature is due to the decreased regularity of the crystallites in the quenched samples.

3.2. Temperature dependence of the storage and loss modulus and the loss factor $\tan \delta$

The storage modulus and the loss factor at 1 Hz of four representative quenched products is shown in Fig. 2 as a function of temperature ((a) $E'(T)$; (b) $\tan \delta(T)$). Below $-50\text{ }^{\circ}\text{C}$ (marked by the broken lines) the differences between the materials, featuring crystallinities between 12 and 67% are small. A small decrease in modulus around $-110\text{ }^{\circ}\text{C}$ is apparent which is caused by the γ -transition being the topic of part III of this article. A significant decrease of the storage modulus with increasing temperature is visible when it reaches values around $1\text{--}2 \times 10^9$ Pa. The corresponding temperatures vary between $-50\text{ }^{\circ}\text{C}$ for LLDPE 11 (crystallinity $x_v = 12\%$) and $50\text{ }^{\circ}\text{C}$ for HDPE 1 ($x_v = 67\%$) (area marked by the dotted lines). In the temperature range between T_m and $(T_m - 80)$ the storage modulus decreases with temperature by almost one decade for all polyethylenes under investigation. As the curves appear to be almost parallel the temperature dependence is similar for all polymers (pentagonal area).

Fig. 2 (right) shows the loss factor $\tan \delta$ as a function of temperature for those samples. The α -relaxation is evident as a distinct shoulder around $80\text{ }^{\circ}\text{C}$ in HDPE 1 while LLDPE 1 shows a broader shoulder around the same temperature. The β -transition is clearly visible for LLDPE 10 and 11 around $-25\text{ }^{\circ}\text{C}$ whereas HDPE 1 and LLDPE 1 show no transition around that temperature. The γ -transition of all samples can be observed as a maximum around $-115\text{ }^{\circ}\text{C}$. In this plot, however, no α' -transition is found. A plot of the loss modulus E'' as a function of temperature increases

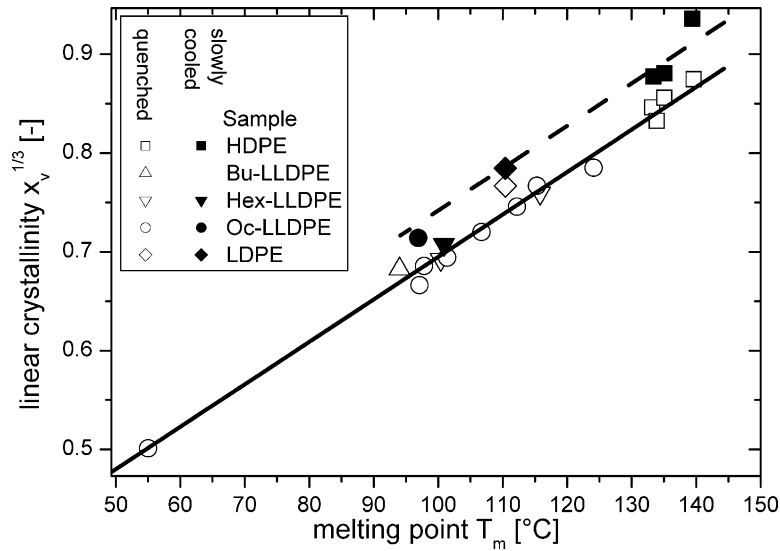


Fig. 1. Dependency of the linear crystallinity on the melting point.

the visibility of the β -transition but reduces the visibility of the γ -transition.

To analyze the influence of crystallinity on the storage modulus at temperatures above the β -transition a model of semi-crystalline polymers is used. In this temperature range two phases exist with a very different behavior: the amorphous phase, being already in the rubbery state, and the crystalline one which has a very high modulus compared to the amorphous phase (\approx factor 1000 (glassy modulus/rubbery modulus)). Therefore, the storage modulus has to be strongly dependent on the crystallinity. To prove this a representative temperature of 60 °C was chosen. This temperature is well above the glass transition temperature which is attributed to the β - or γ -transition both lying distinctly below 0 °C for all samples under investigation. It is still low enough to investigate all samples below their melting point. At this temperature the storage modulus of the samples is linearly dependent on the crystallinity (Fig. 3). This relation can be used to extrapolate the storage modulus

to that for a completely amorphous polyethylene/ α -olefin-copolymer (which would feature a comonomer content of approximately 20 mol% [21]). From Fig. 3 a value of 3×10^6 Pa is obtained at 60 °C. Eq. (3) allows the entanglement molar mass M_e to be calculated.

$$M_e = \frac{3N_L \rho k T}{E} \quad (3)$$

ρ , density at 60 °C (g/cm^3), 0.837 g/cm^3 (calculated with a typical thermal expansion coefficient for rubbery polymers based on ρ (20 °C)=0.854 g/cm^3 for an amorphous polyethylene); N_L , Avogadro–Loschmidt number, $6.022 \times 10^{23} \text{ cm}^{-3}$; k , Boltzmann constant, $1.38 \times 10^{-23} \text{ J/K}$; T , temperature, 333 K; E , extrapolated E -modulus at 333 K and 1 Hz, $E' \approx 3 \times 10^6 \text{ Pa}$; M_e , entanglement molar mass (g/mol).

The entanglement molar mass M_e was calculated to 2300 g/mol . As the SCBs do not contribute to the entanglements because they are too short, the important

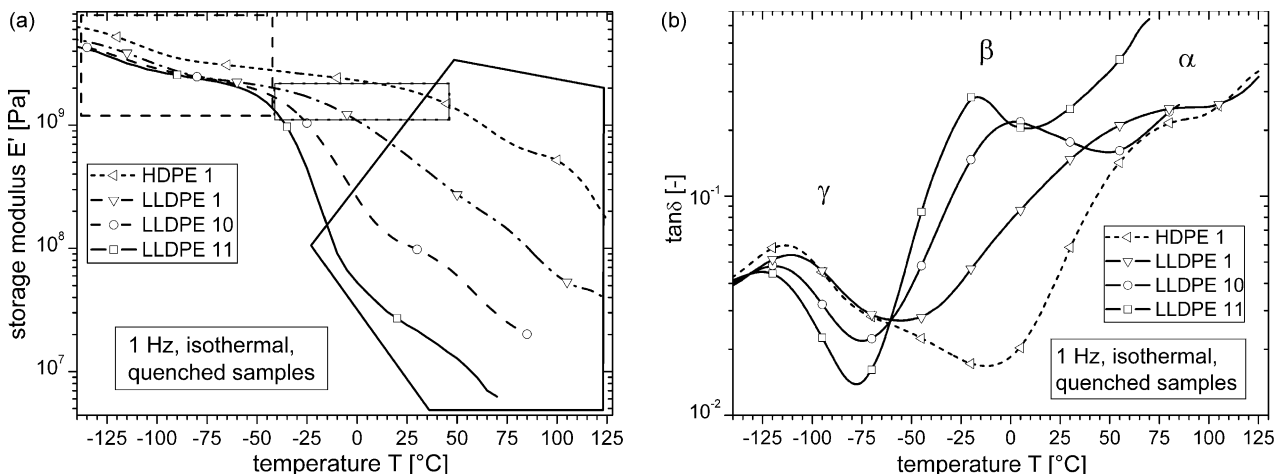


Fig. 2. Temperature dependence of E' (a) and $\tan \delta$ (b) for four selected polyethylenes.

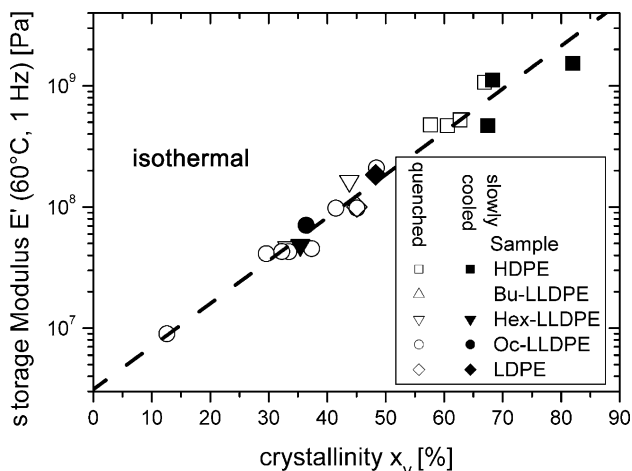


Fig. 3. Dependency of the storage modulus on the crystallinity.

quantity is the molar mass of the backbone. It can be calculated by subtracting the total molar mass of the SCBs from M_e thus leading to a value of 1450 g/mol. This value would be expected for a HDPE (without any comonomer). When comparing the resulting M_e of 1450 g/mol to values obtained by rheological measurements (930–1300 g/mol, [15–17]) the extrapolation gives reasonable values but is a little bit too high.

However, the SCBs will also slightly increase the chain stiffness. Therefore, M_e of a polyethylene without comonomer has to be somewhat lower than 1450 g/mol.

3.3. α' -Relaxation

Generally, it is very difficult to detect the α' -relaxation from the temperature dependence of the loss factor or loss modulus at a fixed frequency (Fig. 4). For HDPE 1 a shoulder is found in the plot $E''(T)$ but the other samples show only very weak traces of the α' -transition. This is due to the fact that the α' -relaxation partly coincides with the α -relaxation and the melting. Only the analysis of the

frequency dependence of the loss factor $\tan \delta(\omega)$ does show the presence of the α' -transition for many samples. The maximum frequency of $\tan \delta$ was taken as a measure for the α' -relaxation.

Two typical examples of α' -transitions are shown in Figs. 5 and 6 for a LDPE and a HDPE, respectively. The maximum of $\tan \delta$ indicating the transition temperature is marked. The shape of the function of the loss factor $\tan \delta$ as a function of frequency, however, looks quite different. The LDPE has a melting point T_m at 110 °C—approximately 80 K above the α' -transition temperature. No α -transition is observed in LDPE 1. Thus, the α' -relaxation is not in the vicinity of any other relaxation (the β -relaxation is the closest relaxation with a transition temperature about 40 K below the α' -transition). Therefore, this transition has a constant peak height of about $\tan \delta = 0.19$.

For the HDPE on the other hand the transition is just below the melting point (about 5–40 K) on one hand and on the other just above the α -transition which is taking place around 40 K below the α' -transition (Fig. 4). As these two transitions have a much higher intensity the weak α' -relaxation is barely observable. The low temperature flank of the melting peak increases the maximum of the α' -relaxation from 0.25 to 0.3.

With increasing proximity to the melting point the maxima of the α - and the α' -relaxations appear to be stacked over each other. This is due to the overlap of the α' -transition-peak and the beginning of the melting peak. This becomes evident as at the melting peak $\tan \delta$ increases dramatically in the temperature range around the α' -relaxation of highly crystalline HDPE.

From the maximum frequencies ν_{\max} at different temperatures the activation energies can be calculated if they follow the Arrhenius Eq. (4).

$$\nu_{\max}(T) = \nu_0 \exp\left(-\frac{E_a}{RT}\right) \quad (4)$$

E_a , activation energy (kJ/mol); R , gas constant.

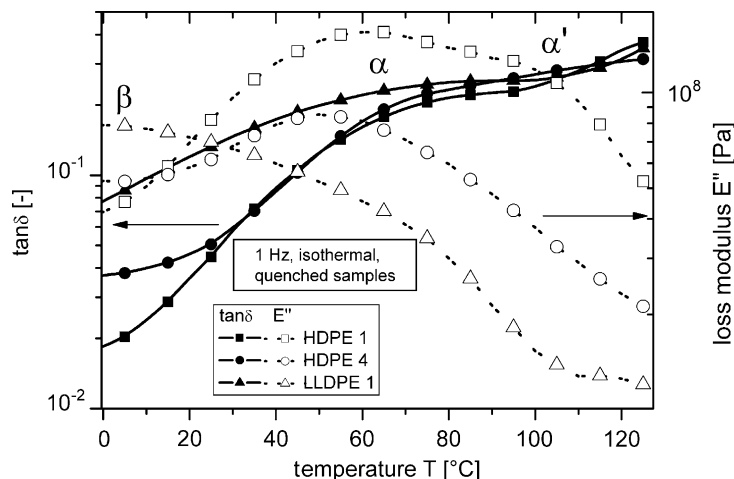


Fig. 4. Temperature dependence of $\tan \delta$ (left y-axis) and E'' (right y-axis) of three quenched samples.

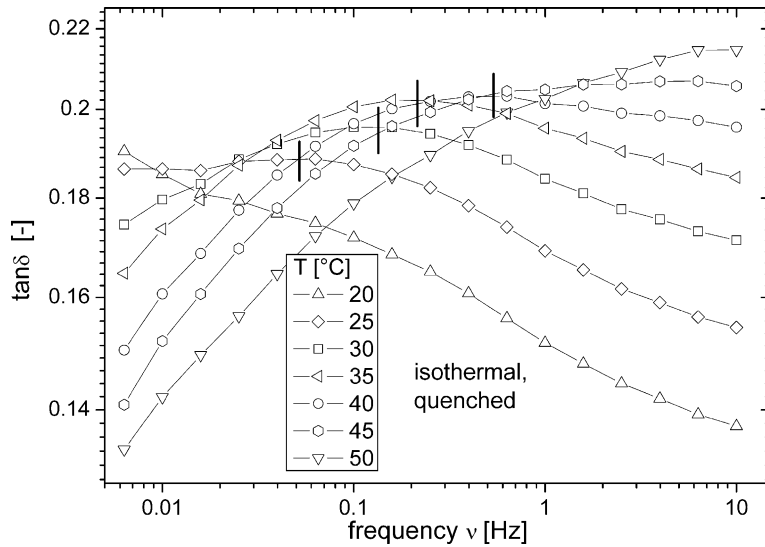


Fig. 5. α' -relaxation of quenched LDPE 1.

The Arrhenius plots of several products are shown in Fig. 7. The Arrhenius plots are depicting the broad temperature range in which the α' -relaxation occurs. This is due to the broad range of crystallinities down to 40%.

As discussed above different morphologies are known for polyethylene with different crystallinities. The samples shown in Fig. 7 possess lamellar type III and IV-morphologies according to the polyethylene morphology scheme [18]. The crystal lamella thickness l_c varies over a broad range while the interlamellar thickness l_a stays approximately constant (10.5 nm) [2]. Therefore, the structure of the interfacial region should also exhibit a great variety. All α' -transitions were observed in products with more than 40% crystallinity, which approximately is the border between lamella and bundle crystallite dominated microstructures [18]. Thus, it is concluded that the α' -

relaxation is related to interface processes in the crystal lamellae [2,7,15].

The activation energies found are in the range between 37 and 145 kJ/mol (cf. Table 3). As a general trend the activation energy decreases with increasing α' -relaxation temperature. Further discussions on the activation energies of the α' -transition will be found later.

We postulate that the activation energy and the transition temperature depend on the thickness of the lamellae in the crystals. As it is complicated to directly measure the dimensions of the crystal lamellae an indirect measure for the lamella thickness has to be found. Again the linear crystallinity is used, which is assumed to be—as stated above—proportional to the dimensions of the crystal lamellae. To compensate for the different temperatures of the α' -relaxations with are due to the different melting

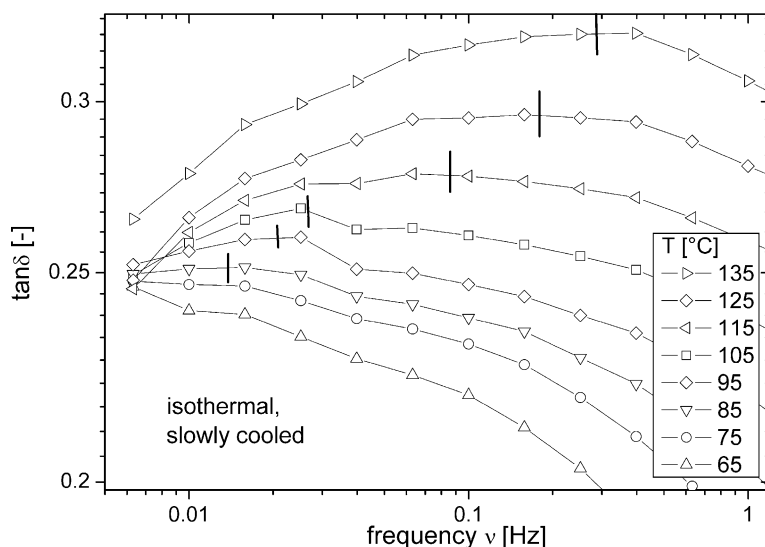


Fig. 6. α' -relaxation of slowly-cooled HDPE 1.

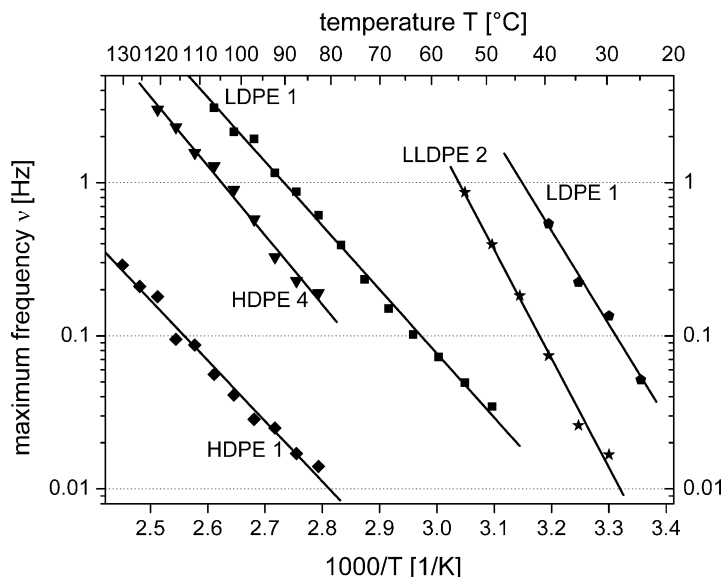


Fig. 7. Arrhenius-plots of the α' -relaxations of different polyethylenes.

Table 3
Activation energy and relaxation temperature at 0.1 Hz of the α' -relaxations

Name	Quenched samples			Slowly-cooled samples		
	Crystallinity x_v (%)	Activation energy α' -relaxation (kJ/mol)	$T \alpha'$ (0.1 Hz) (°C)	Crystallinity x_v (%)	Activation energy α' -relaxation (kJ/mol)	$T \alpha'$ (0.1 Hz) (°C)
HDPE 1	70	52	85	80	75	118
HDPE 2	61	75	67	68	37	— ^a
HDPE 3	63	99	83	68	66	— ^a
HDPE 4	58	136	77			
LLDPE 1	48	83	60			
LLDPE 2	45	136	41			
LDPE 1	45	117	29	48	80	62
LLDPE 3	44	145	40			
LLDPE 4	42	99	29			
LLDPE 5–11	No α' -transition observed					

^a No meaningful value (above T_m).

temperatures a relative α' -transition temperature ($T_m - T_{\alpha'}$) is defined.

By plotting $T_m - T_{\alpha'}$ vs. $x_v^{1/3}$ (Fig. 8) and $E_a^{\alpha'}$ vs. $x_v^{1/3}$ (Fig. 9) a closer investigation of the underlying molecular processes is possible. The plot $T_m - T_{\alpha'}$ vs. $x_v^{1/3}$ clearly indicates that the α' -transition moves more closely to the melting peak with increasing crystallinity. By extrapolating the data to 100% crystallinity it can be shown that the α' -transition merges with the melting peak and thus disappears completely. The same tendency is found in the plot of the activation energy $E_a^{\alpha'}$ vs. $x_v^{1/3}$ where the activation energy for the α' -process tends to zero for a completely crystalline product. The error in the activation energy was found to be around 5% (uncertainty of the fit routine). Error bars for one sample are drawn in Figs. 8 and 9 to show the high accuracy of the measurements.

These results indicate that the α' -transition occurs as long as the crystal structure is lamellar and no completely

crystalline structure is achieved. When the crystallinity approaches 100%, all interfaces between lamellar and amorphous regions will disappear. Thus the α' -relaxation will disappear.

On the other hand, when the distortions of the crystal structure by the SCB are too dominant to produce a lamella dominated microstructure the α' -transition disappears, too.

It is also interesting to note that the α' -relaxation temperature increases linearly with the melting temperature for the quenched samples (Fig. 10). The α' -relaxation temperature of the two slowly cooled samples that show reliable values² are shifted to 31 K higher values than the quenched ones. This is an indication of the strong

² Slowly-cooled HDPE 2 and 3 show extrapolated values significantly above T_m , which is physically not meaningful. The α' -relaxations of these samples are only observed in a very narrow frequency range very close to the melting point, thus the extrapolation of these values is questionable.

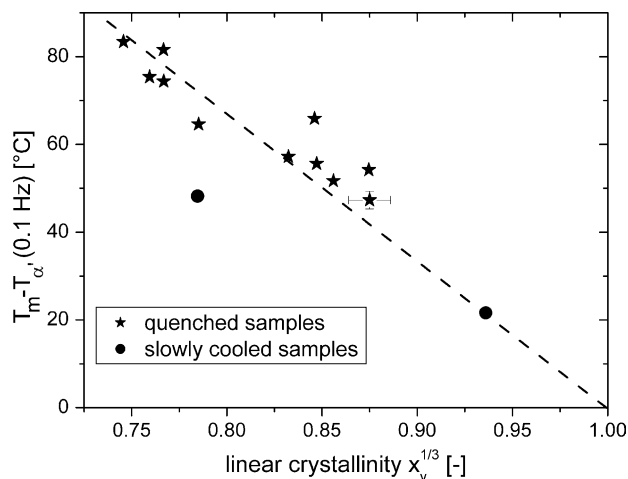


Fig. 8. $T_m - T_{\alpha'}$ of the α' -relaxations as a function of $x_v^{1/3}$ for different polymers.

dependence of the interface structure on the cooling conditions as described by Nitta and Tanaka [2] and Matthews et al. [3]. As the slowly-cooled samples have a much longer time for crystallization their interface region should be much smaller than the one of the quenched samples. This may explain the strong influence of the cooling conditions on the α' -relaxation. A higher ordered interface will increase the relaxation temperature significantly. This is found for the samples under investigation by the increase of the α' -relaxation temperature of 31 K.

The activation energy is a measure of the potential barrier hindering the molecular motion. The disappearance of any disordered phase in completely crystalline samples means that there is no relaxation process to take place. As the boundary between the crystal lamellae and the amorphous phase is not sharp but gradual the crystallization also influences the crystal-amorphous interface region. Incorporation of a comonomer will lower the crystallinity. Therefore, samples containing comonomers feature areas of incomplete crystallization, i.e. partially ordered interface, at

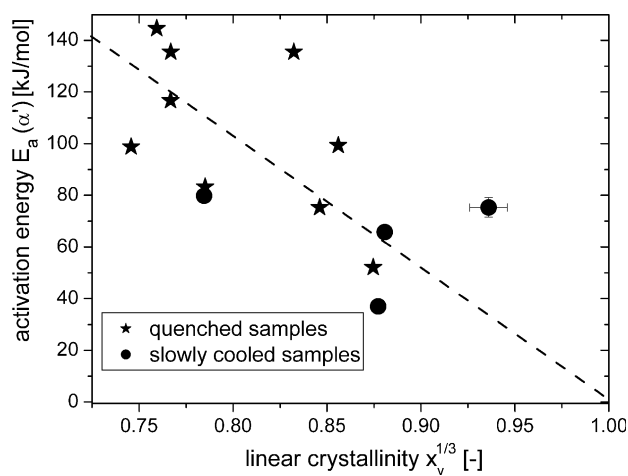


Fig. 9. Activation energies of the α' -relaxations as a function of $x_v^{1/3}$ for different polymers.

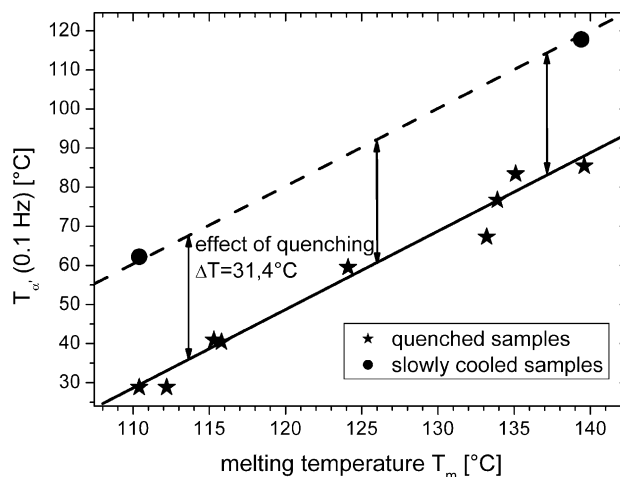


Fig. 10. $T_{\alpha'}$ of the α' -relaxations as a function of T_m for different polymers.

the borders of the lamellae. This crystal–amorphous interface is determined by these areas of incomplete crystallization. These tendencies are summarized schematically in Fig. 11.

As in the very thin layer of the interface for a highly crystalline sample the relaxation is much more sterically hindered by the stiff lamellae than in the more gradual interface of a sample with a lower crystallinity the α' -relaxation has to move more closely to the melting point T_m to occur.

Therefore, it is concluded by us as well as by Nitta and Tanaka [2], Takayanagi and Matsuo [7] and Matthews et al. [3] that the α' -transition is a relaxation process which is taking place in the partially-ordered interface between the lamellae and the amorphous regions. This interfacial region becomes increasingly ordered and smaller when the fully crystalline state is approached. This is the explanation why no α' -transition exists for 100% crystalline samples.

These findings agree with Nitta and Tanaka [2], Matthews et al. [3], and Takayanagi and Matsuo [7].

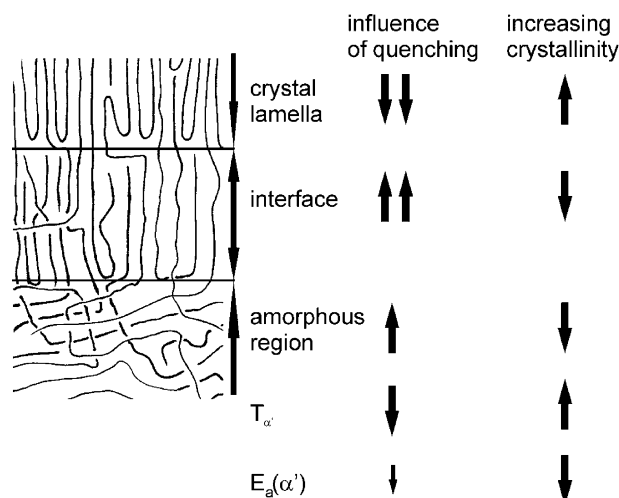


Fig. 11. Scheme of the influence factors of the α' -relaxation.

The proximity to the melting peak suggests that the molecular process behind the α' -transition is the glass transition of the sterically hindered interfacial region. The crystallinity influences the interface in two ways. On one hand, a higher crystallinity means that the chains are higher ordered and thus the interface becomes thinner. On the other hand a stronger sterical hindrance will lead to a lower degree of crystallinity and therefore to an increased size of the half-ordered region. Thus increasing the crystallinity will lead to thinner but more ordered interfaces.

As free volume is necessary for any molecular movement a higher degree of order will lead to a smaller free volume in the amorphous phase [21]. In highly ordered interface regions, sufficient free volume can be generated only by thermal expansion (e.g. higher temperature). This picture will explain the rise in $T_{\alpha'}$ with increasing crystallinity.

Incorporation of SCB will lead to an increased free volume which is due to the end group of the SCB. The activation energy on the other hand decreases with increasing α' -transition temperature.

Besides the decrease of the free volume in the interface with increasing crystallinity the local order in this region will increase. Therefore, the potential barrier for molecular movements reflected in the activation energy will decrease because less cooperative motions of neighboring chains are necessary.

4. Conclusions

The α' -relaxation is observed for all examined products with a crystallinity between almost 100 and 40%. Its activation energy declines from 140 to 30 kJ/mol with increasing crystallinity. The activation energy vanishes when extrapolated to a fully crystalline polymer. $T_{\alpha'}$ is increasing with increasing crystallinity.

As the α' -relaxation is only visible in products with a crystallinity between 100 and 40% it is concluded that a lamellar crystal structure (type III and IV) is necessary for the existence of an α' -transition. The decrease of the activation energy with decreasing linear crystallinity can be explained by the increasing perfection of the crystal lamellae. The same effect is observed when looking at the proximity of the α' -relaxation temperature to the melting point ($T_m - T_{\alpha'}$). With increasing crystallinity the difference between the melting point T_m and the α' -transition temperature $T_{\alpha'}$ decreases. For a fully crystalline sample it is expected that T_m and $T_{\alpha'}$ merge. It is, therefore, concluded that the α' -relaxation originates from the interfacial region which disappears in a single crystal.

The interfacial region in which the α' -transition is located can only exist when the crystal structure is lamellar, i.e. when the crystallinity is not too low and not too high to form lamellae. Because of that the α' -relaxation does not

occur at crystallinities where no lamellar structure is possible any more ($x < 40\%$). The most important way of deliberately attaining a non-lamellar morphology is to use comonomers such as α -olefins. The molar mass and the cooling conditions are also influencing the crystallinity although not as much as the comonomer content.

It is also not observable for fully crystalline polymers as single crystals (i.e. infinitely thick lamellae) by definition do not have any interfaces.

The activation energy of the α' -relaxation is a function of the sterical hindrance as well as of the proximity of the α' -relaxation temperature to the melting point which means that the interfacial region becomes smaller with increasing crystallinity.

As the thickness of the lamellae is very small compared to the length and width the linear crystallinity is a simple but effective measure of the lamellae dimensions.

Acknowledgements

The authors want to thank Dipl.-Chem. Mariana Sturm for the spectroscopic measurements and Mrs. Inge Herzer and Dipl.-Ing. Dietmar Auhl for the SEC-MALLS measurements.

References

- [1] Stehling F, Mandelkern L. *Macromolecules* 1970;3:242–52.
- [2] Nitta KH, Tanaka A. *Polymer* 2001;42:1219–26.
- [3] Matthews RG, Ward IM, Capaccio G, Unwin A. *J Macromol Sci, Phys* 1999;B38:123–43.
- [4] Papir YS, Baer E. *J Appl Phys* 1971;42(12):4667–74.
- [5] Hartwig G. *Polymer properties at room and cryogenic temperatures*. NY, USA: Plenum Press; 1994.
- [6] Simanke AG, Galland GB, Freitas L, da Jornada JAH, Quijada R, Mauler RS. *Polymer* 1999;40:5489–95.
- [7] Takayanagi M, Matsuo T. *J Macromol Sci, Phys B* 1967;1:407.
- [8] Bensason S, Nazarenko S, Chum S, Hiltner A, Baer E. *Polymer* 1997;38:3513–20.
- [9] Stadler F, Kaschta J, Münstedt H. In preparation.
- [10] Stadler F, Kaschta J, Münstedt H. In preparation.
- [11] Zimm BH, Stockmayer WH. *J Chem Phys* 1949;17:1301–14.
- [12] Schwarzl F. *Polymermechanik*. Berlin: Springer; 1990.
- [13] Wolf B, Kenig S, Klopstock J, Miltz J. *J Appl Polym Sci* 1996;62:1339–46.
- [14] Kraft M. Dissertation. Zürich: ETH; 1996.
- [15] Jordens K, Wilkes GL, Janzen J, Rohlfing DC, Welche MB. *Polymer* 2000;41:7175–92.
- [16] Luettmer-Strathmann J. *J Chem Phys* 2000;112:5473–9.
- [17] Gabriel C. Dissertation University Erlangen-Nürnberg. Aachen: Shaker Verlag; 2001.
- [18] Bubeck RA. *Mater Sci Eng* 2002;R39:1–28.
- [19] Popli R, Glotin M, Mandelkern L. *J Polym Sci Phys* 1983;21:407–48.
- [20] Struik LCE. *Physical aging in amorphous polymers and other materials*. NY, USA: Elsevier; 1978.